UNIVERSIDAD DE LOS ANDES
Department of Physics

Detection of mammographic lesions using Speckle X-ray Tracking method

C.Tibambre, E. Cely, C.Ávila

Universidad de los Andes | Facultad de Ciencias | Departamento de Física
2024
Workshop on Particle Detectors for Interdisciplinary Applications.
September 30 – October 2.
Official Language: Spanish/English.
Idioma Oficial: Español/Ingles.

Outline

Motivation

Breast Cancer Nowadays

According with the **World Health Organization:**

- Breast cancer caused 670 000 deaths globally in 2022.
- Roughly half of all breast cancers occur in women with no specific risk factors other than sex and age.
- Breast cancer was the most common cancer in women in 157 countries out of 185 in 2022.
- Breast cancer occurs in every country in the world.
- Approximately 0.5–1% of breast cancers occur in men.

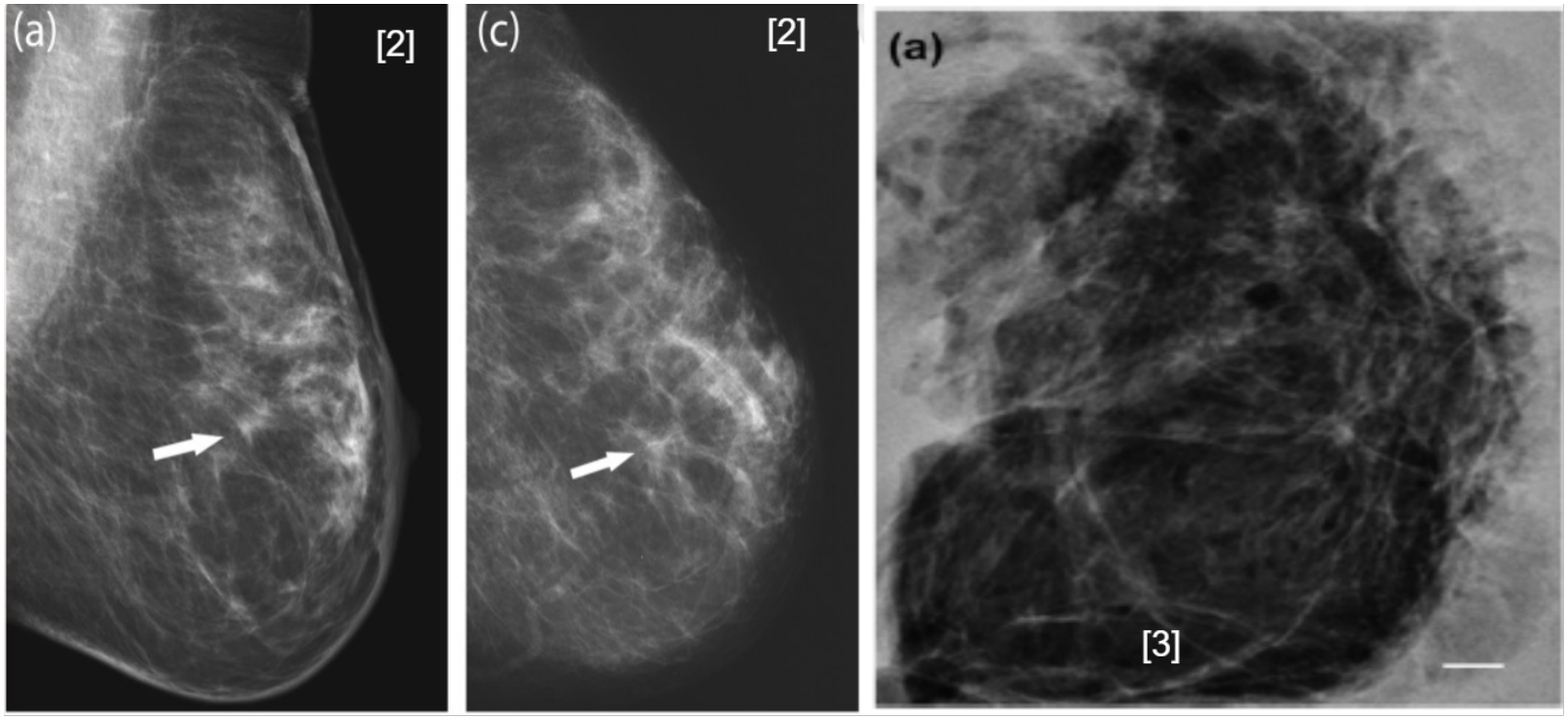

Propagation-based imaging mammograms recorded at a synchrotron source and clinical mamogram [2],[3].

Motivation

Phase contrast detection

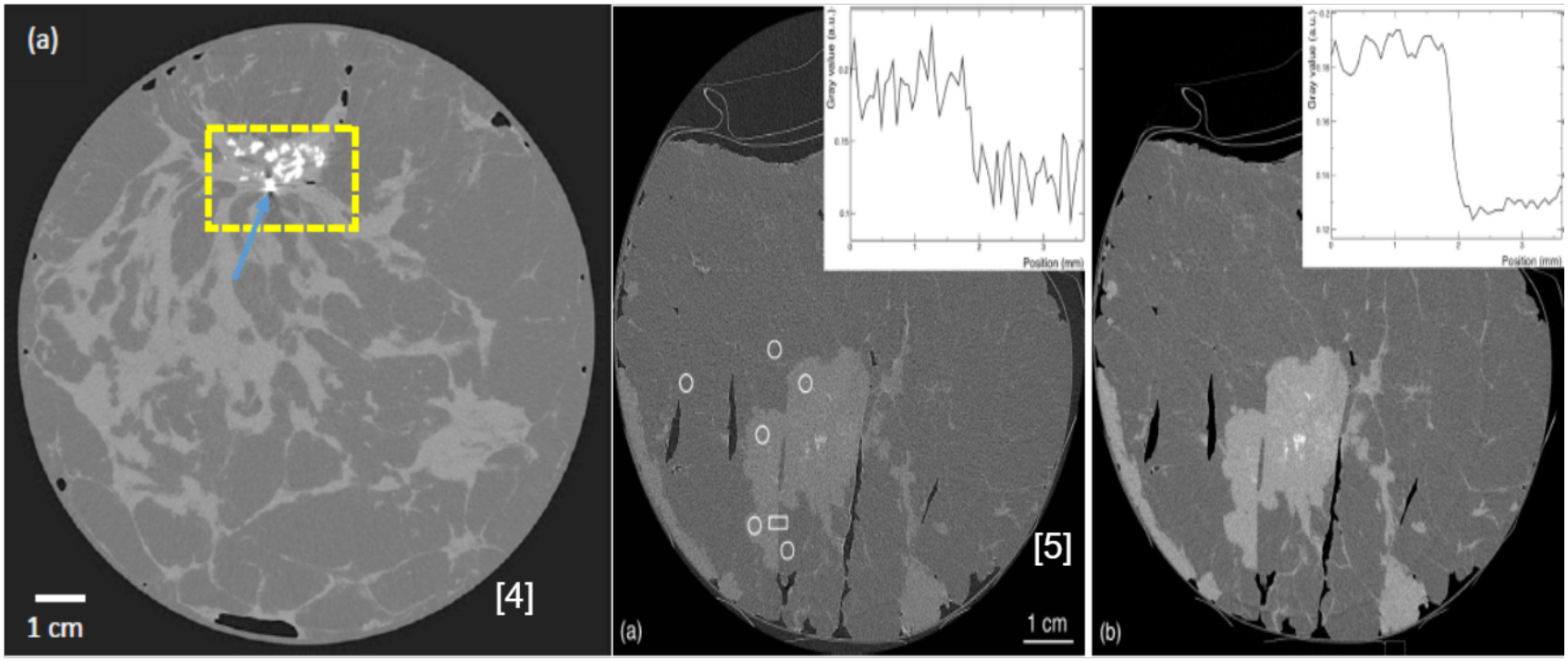

Phase contrast images using CT [4],[5].

$$\psi_{out}(x,y,\omega) = \psi_{in}(x,y,\omega)e^{ikz}e^{-\int k\beta(x,y,z,\omega)dz}e^{-\int ik\delta(x,y,z\omega)dz} \quad (1)$$

$$n(x,y,z,\omega) = 1 - \delta(x,y,z,\omega) + i\beta(x,y,z,\omega) \quad (2)$$

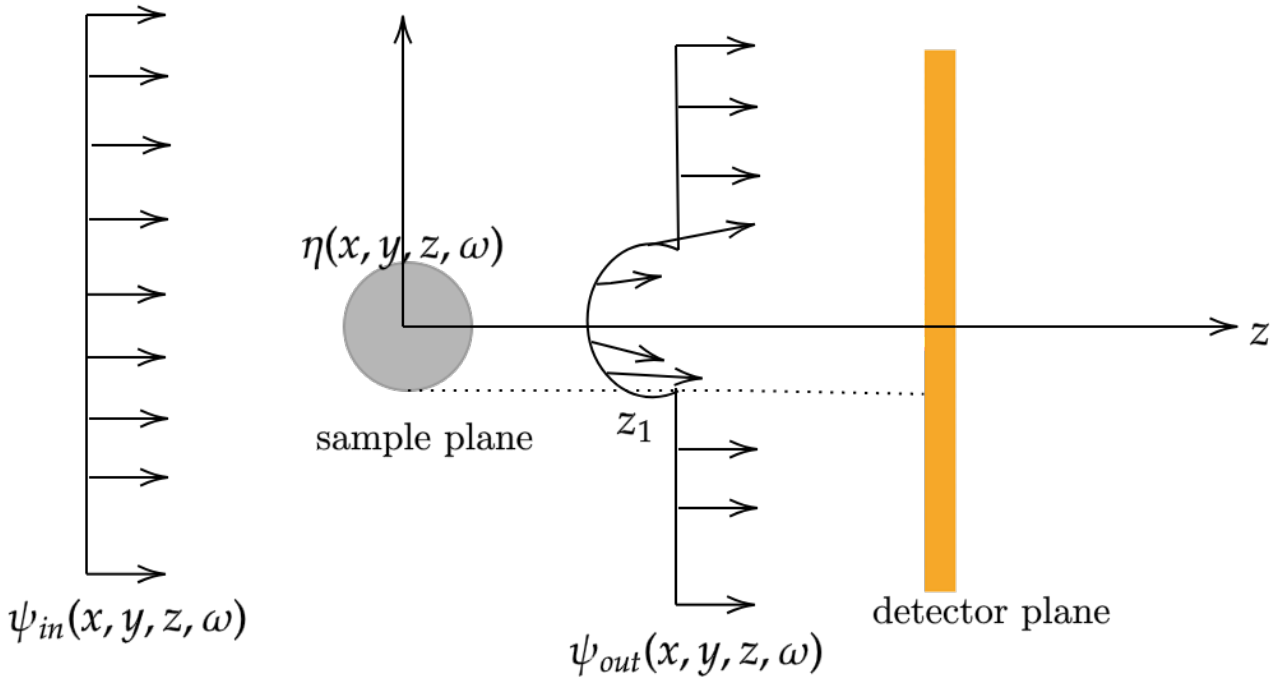

schematic description of X-rays interacting with matter.

Theoretical framework
Absorption and phase shift

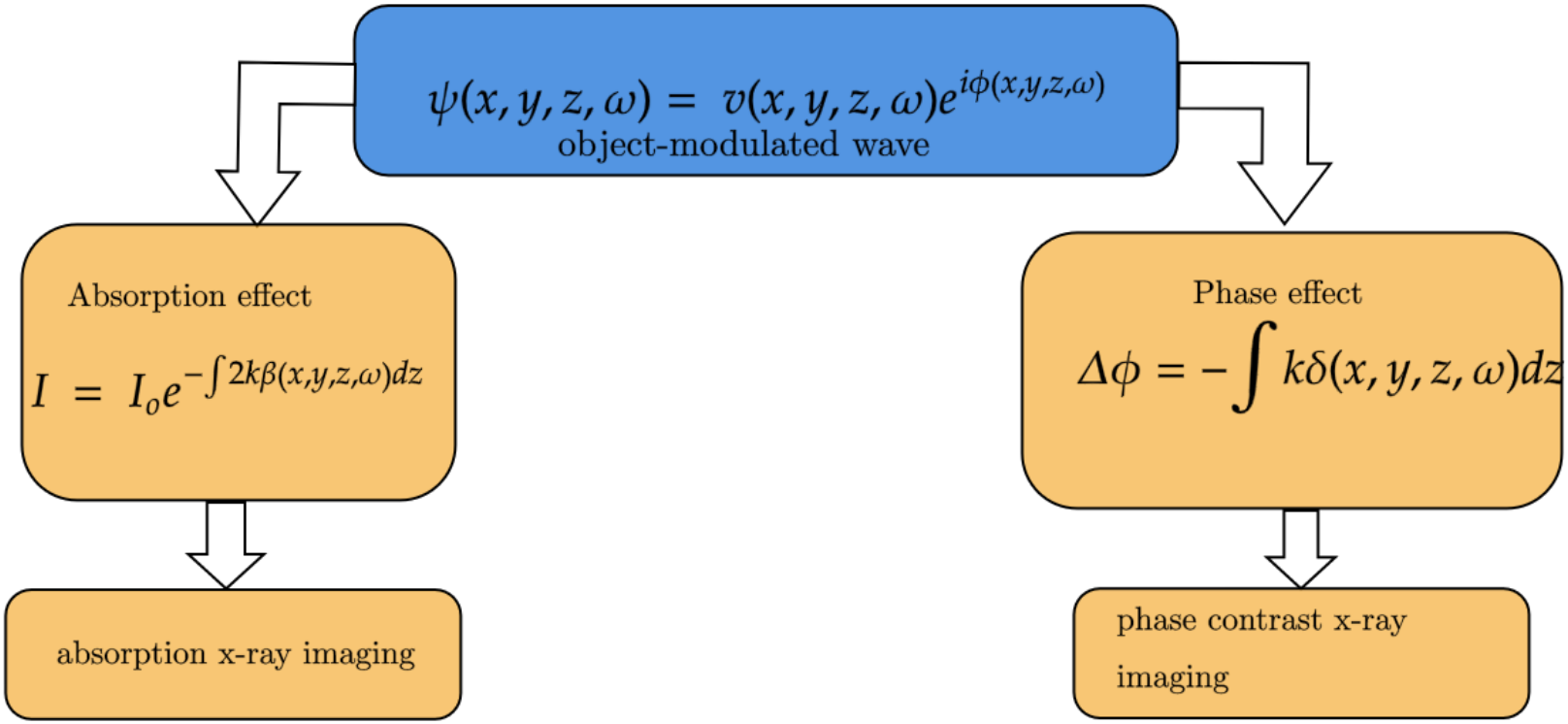

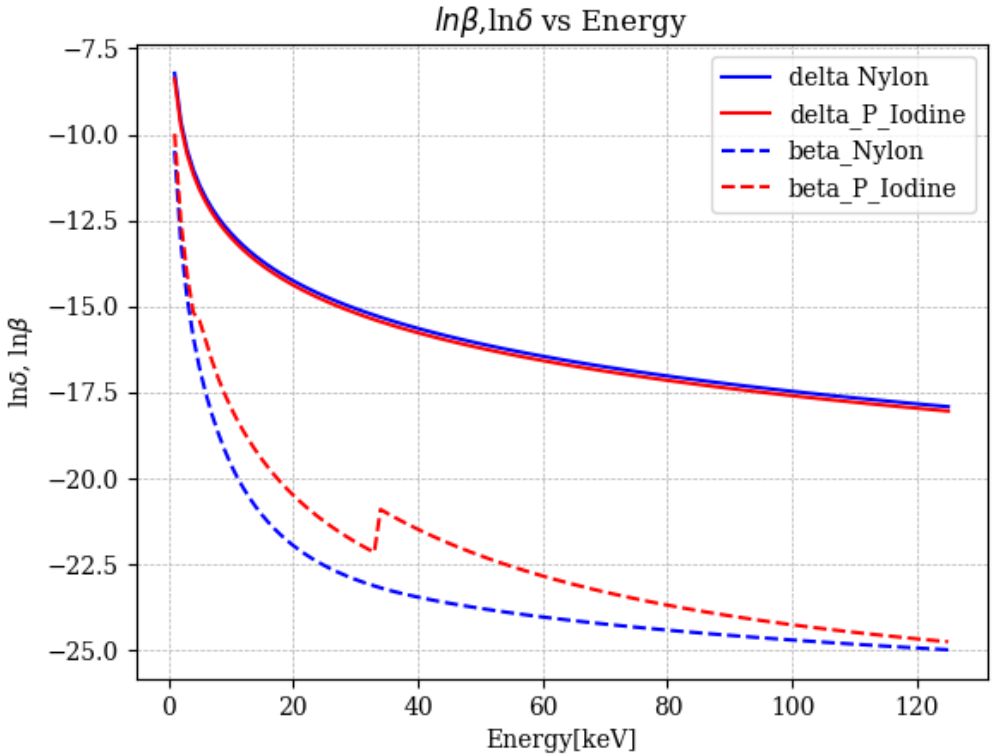

For soft materials at energies $5keV < E < 60keV$:

$$\frac{\delta}{\beta} \approx 10^3 \quad (3)$$

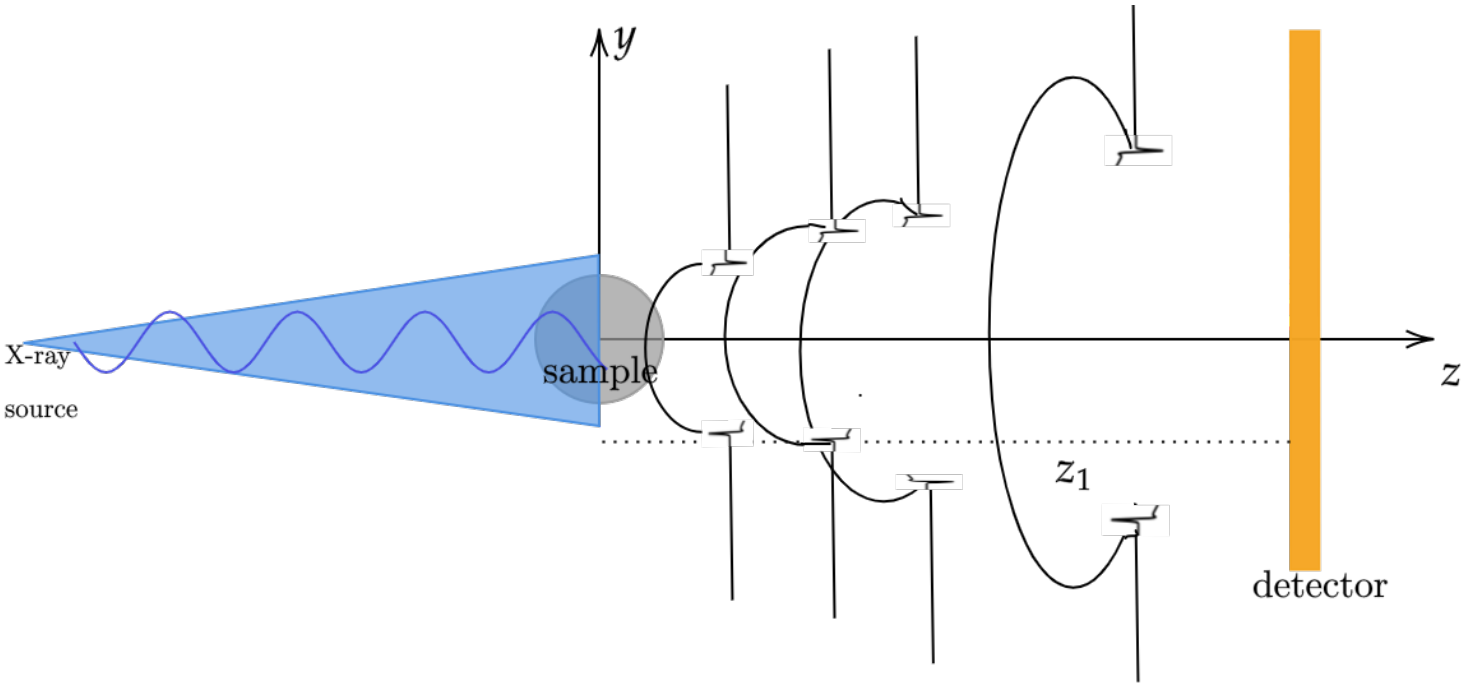

Experimental realization of In-line PCI X-ray imaging

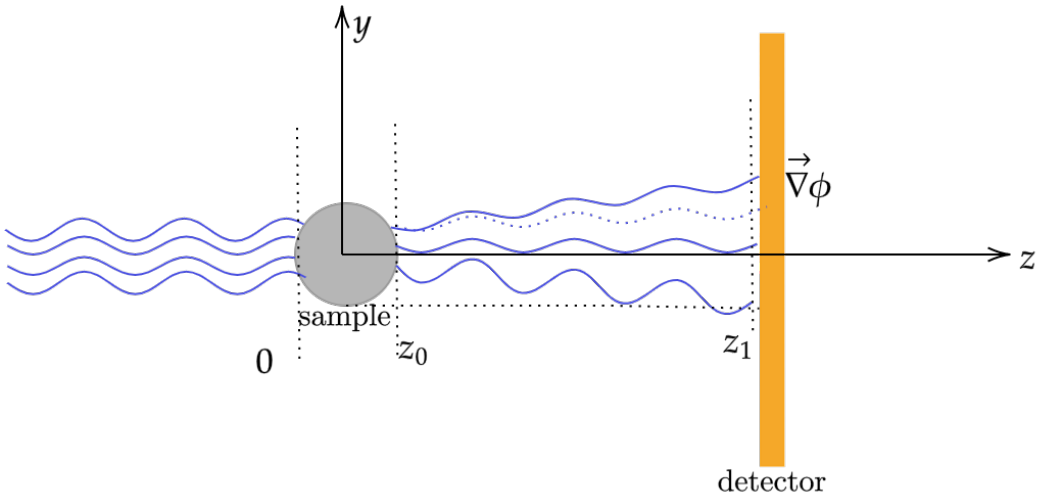

From Transport Intensity Equation:

$$\frac{I(x,y,z=z_1,\omega)}{I(x,y,z=z_0,\omega)} = 1 - \frac{z_1}{k}\nabla_\perp^2 \Delta\phi(x,y,z_0,\omega) \tag{4}$$

Applying phase retrieval methods(Paganin Algorithm):

$$\Delta\phi(x,y,z=z_1,\omega) = \frac{\gamma}{2} ln\left(\mathscr{F}^{-1}\left\{\frac{\mathscr{F}(f(x,y,z=z_1,z_0,\omega))}{1+\frac{z_1\gamma}{2k_o}(u^2+v^2)}\right\}\right) \tag{5}$$

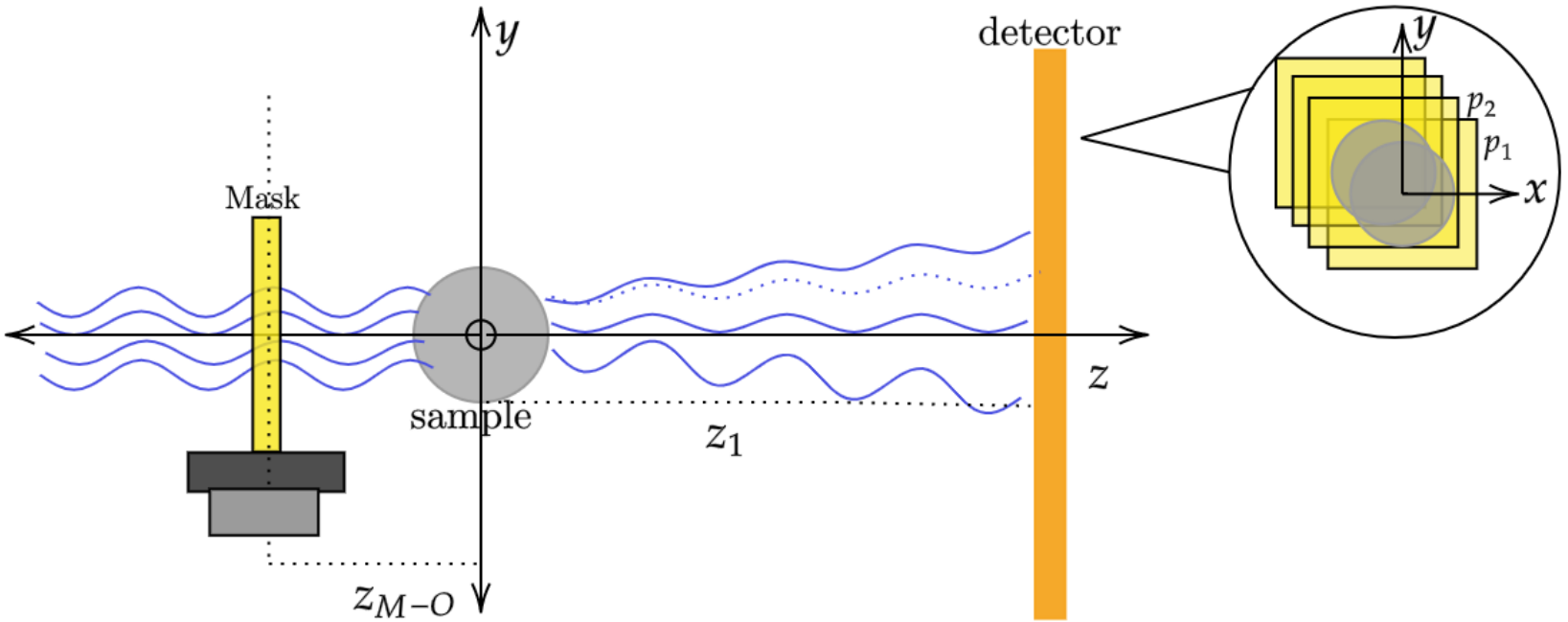

Experimental realization of the SBI method

Each speck works as a beam marker, depending on the method to retrieve the phase signal the way to collect the sample and reference image would change.

Construct a cost function:

$$f(x_0.y_0, \delta_x, \delta_y, T, DF) = \int [T(I_0 + DF\Delta I_r(x-\delta_x, y-\delta_y)) - I(x,y)]^2 \times w(x-x_0, y-y_0)dxdy \tag{6}$$

Minimizing over T and DF variables:

$$T = \frac{\bar{I}(w * \Delta I_r^2) - (w * \Delta I_r)((wI) * r)}{I_o((w * \Delta I_r^2) - (w * \Delta I_r))^2} \tag{7}$$

$$DF = \frac{1}{T} \frac{(wI) * \Delta I_r - \bar{I}(w * \Delta I_r)}{(w * \Delta I_r^2) - (w * \Delta I_r)^2)} \tag{8}$$

Where the convolution * can be written as:

$$w * \Delta I_r = \int w(x - x_o, y - y_o)\Delta I_r(x - \delta_x, y - \delta_y)dxdy \tag{9}$$

Regarding that visibility ($\nu = 20\%$)

From the Fokker-Plank equation:

$$I_R(\mathbf{r}) - I_S(\mathbf{r}) = \frac{z_1}{k}\nabla_\perp \cdot [I_R(\mathbf{r})\nabla_\perp \phi_{obj}] - z_1\nabla_\perp^2[D_{eff}(\mathbf{r})I_R(\mathbf{r})]. \tag{10}$$

At least it is necessary to collect four samples and reference images.

$$D_{eff,phase}(\mathbf{r}) = \mathscr{F}^{-1}[e^{-\rho(k_x^2+k_y^2)}\,\mathscr{F}(D_{eff}(\mathbf{r})) + \frac{1-e^{-\rho(k_x^2+k_y^2)}}{ik_x - k_y}\mathscr{F}(D_{eff}^x(\mathbf{r}) + iD_{eff}^y(\mathbf{r}))] \tag{11}$$

$$\phi_{obj} = \nabla_\perp^{-2}[\frac{k}{z_1 I_R}(\mathbf{r})(I_R(\mathbf{r}) - I_S(\mathbf{r}) + z_1\nabla_\perp^2[D_{eff}I_R(\mathbf{r})]] \tag{12}$$

Where:

$$\nabla_\perp^{-2} = -\mathscr{F}^{-1}\frac{1}{k_x^2+k_y^2}\mathscr{F}, \tag{13}$$

Mammography setup

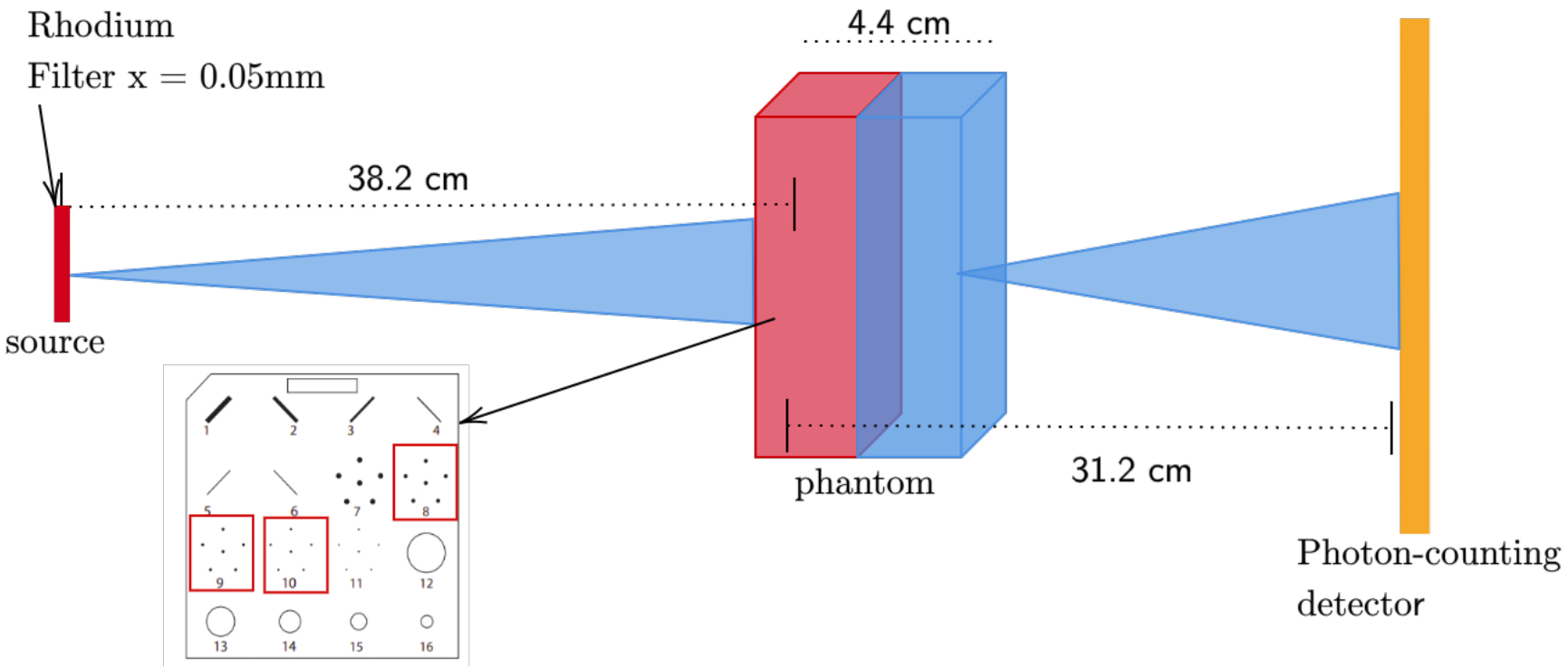

Experimental setup for data acquisition in conventional mammography using 28kVp and 50μA

Experimental setup

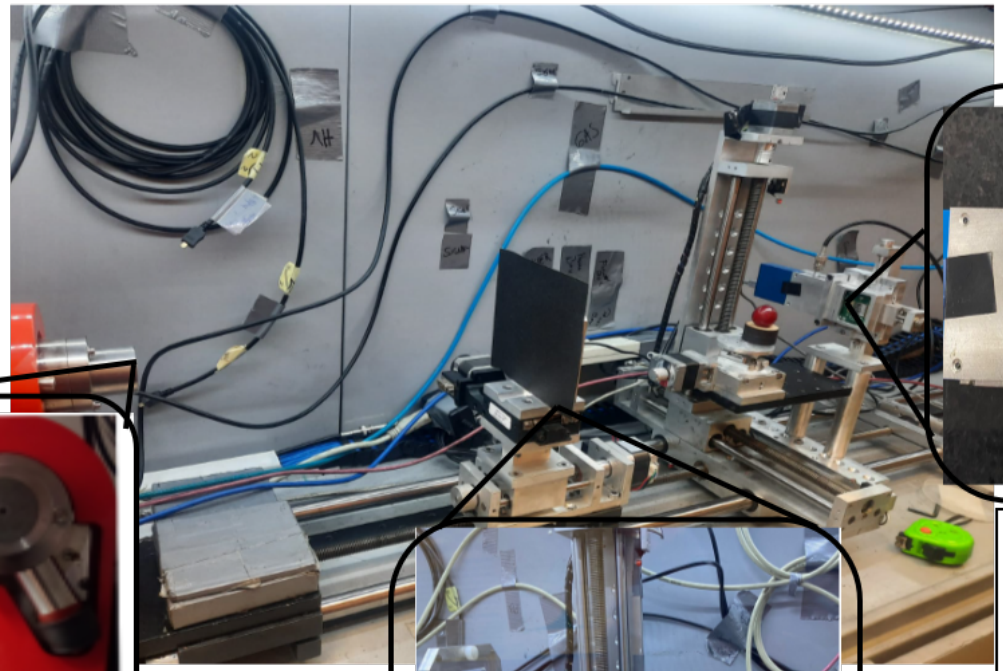

Microfocus X-ray source with a Be window and W anode.

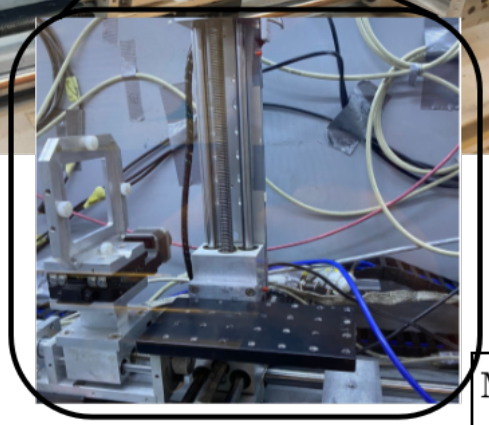

Micrometric motor and support to the abrasive material.
Effective step = 3um

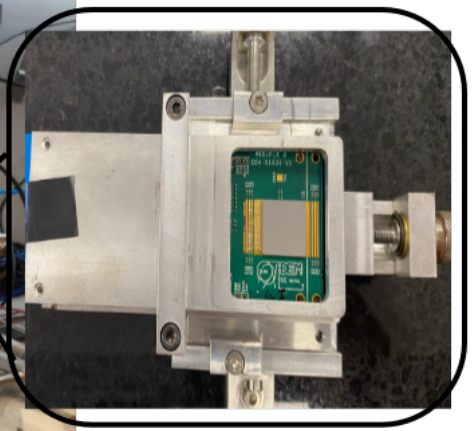

Medipix3RX detector:
256x256 pixels.
300 um Si as sensor.

Timepix3 detector

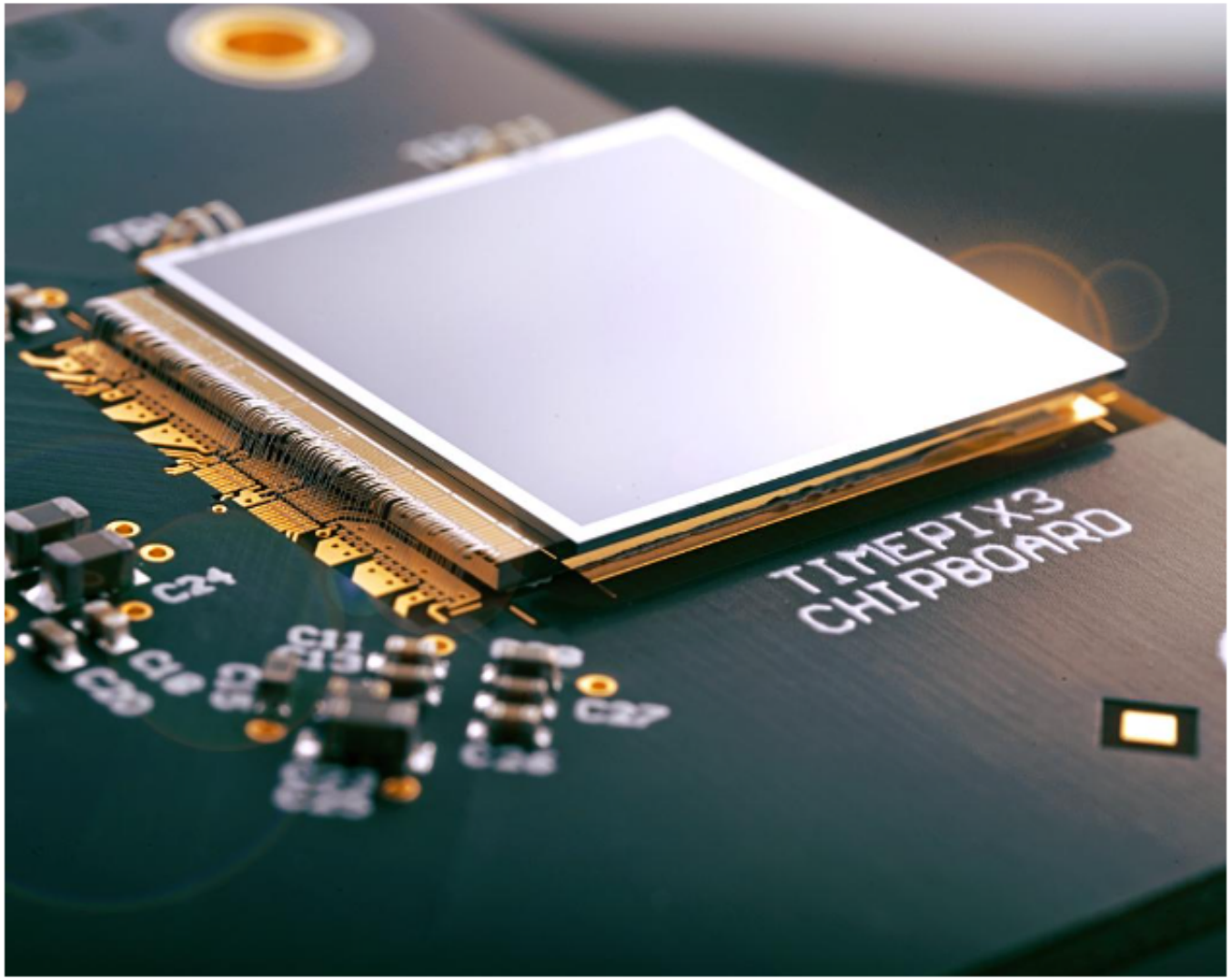

Timepix3 detector
Scheme of matrix pixels

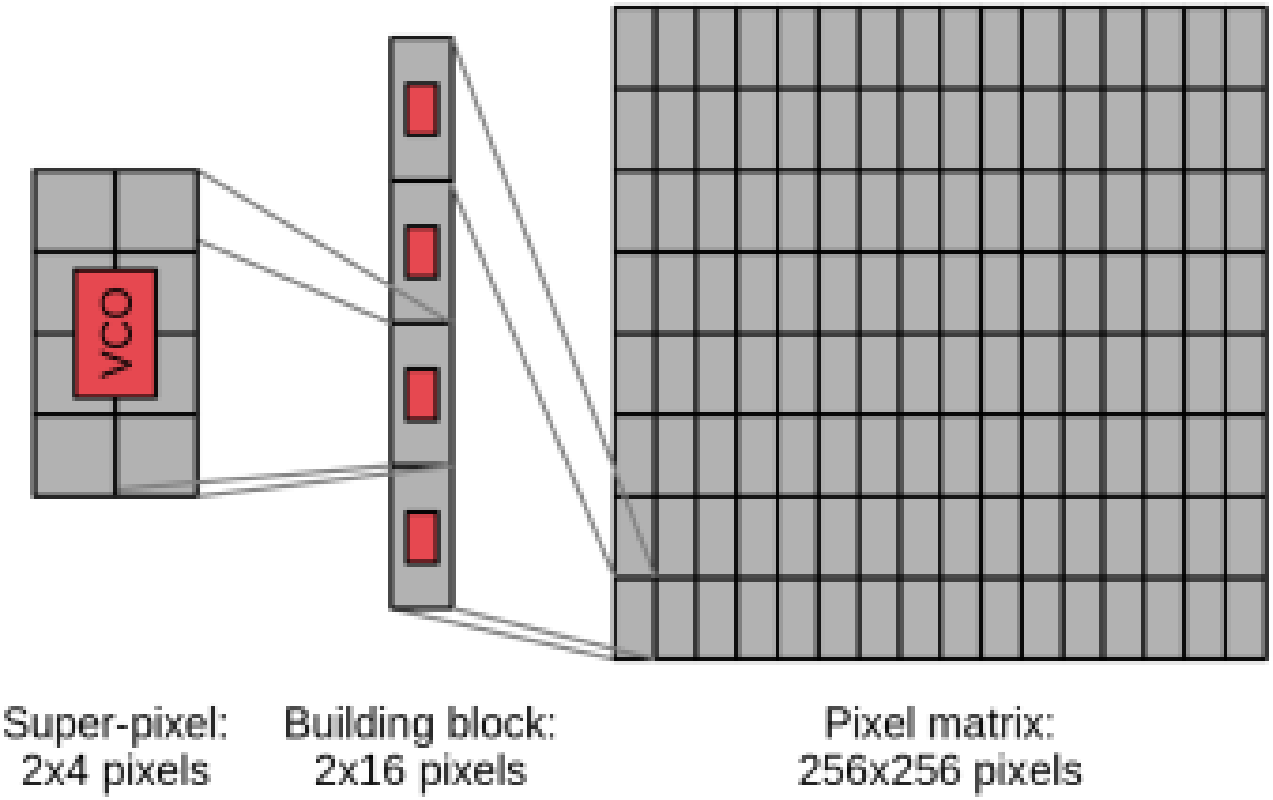

The structure of the pixel matrix.
source : *DialingbacktimeonTimepix*3, *Msc*.*Thesis*.*RobbertGeertsema*

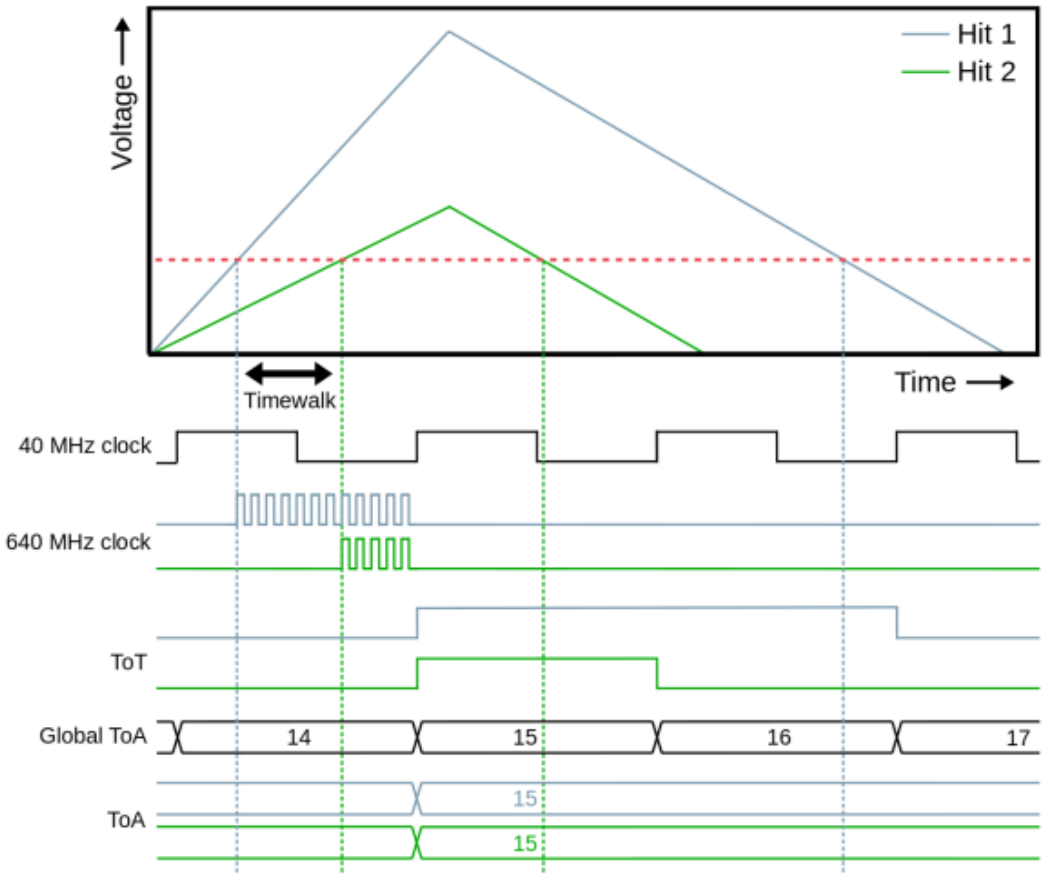

ToT and ToA detection. *source* : *DialingbacktimeonTimepix3, Msc.Thesis.RobbertGeertsema*

Geant4 and PEPI project

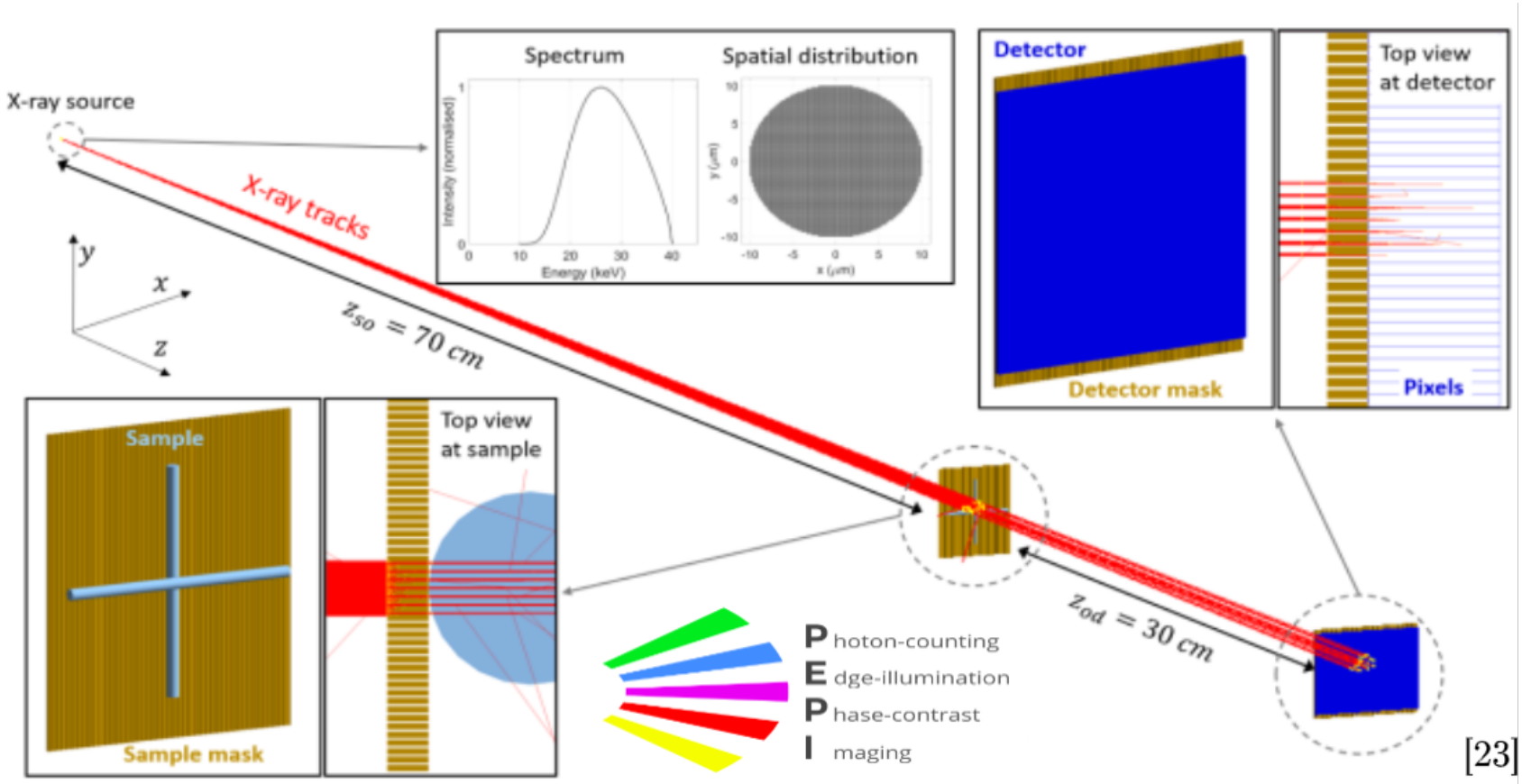

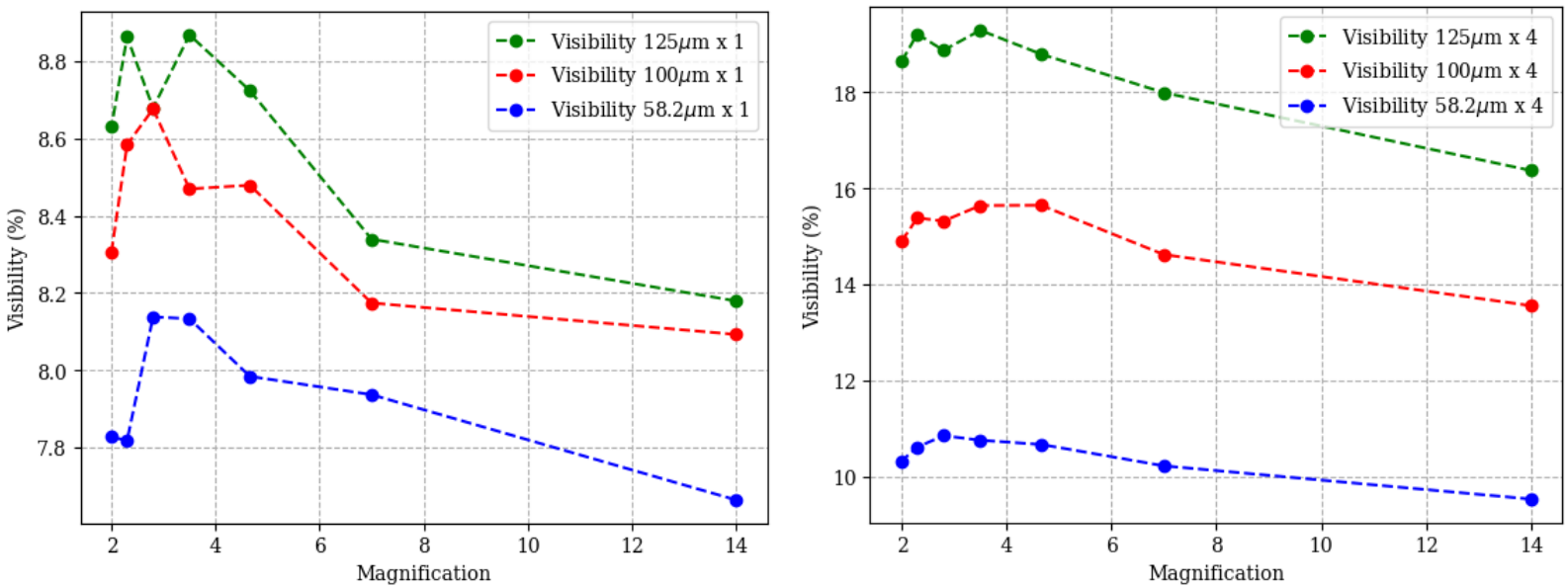

left: Visibility curve using one sandpaper. **right:** Visibility curve using four sandpapers

$$\nu = \frac{\sigma_I}{\bar{I}} \tag{14}$$

Cut-off optimization

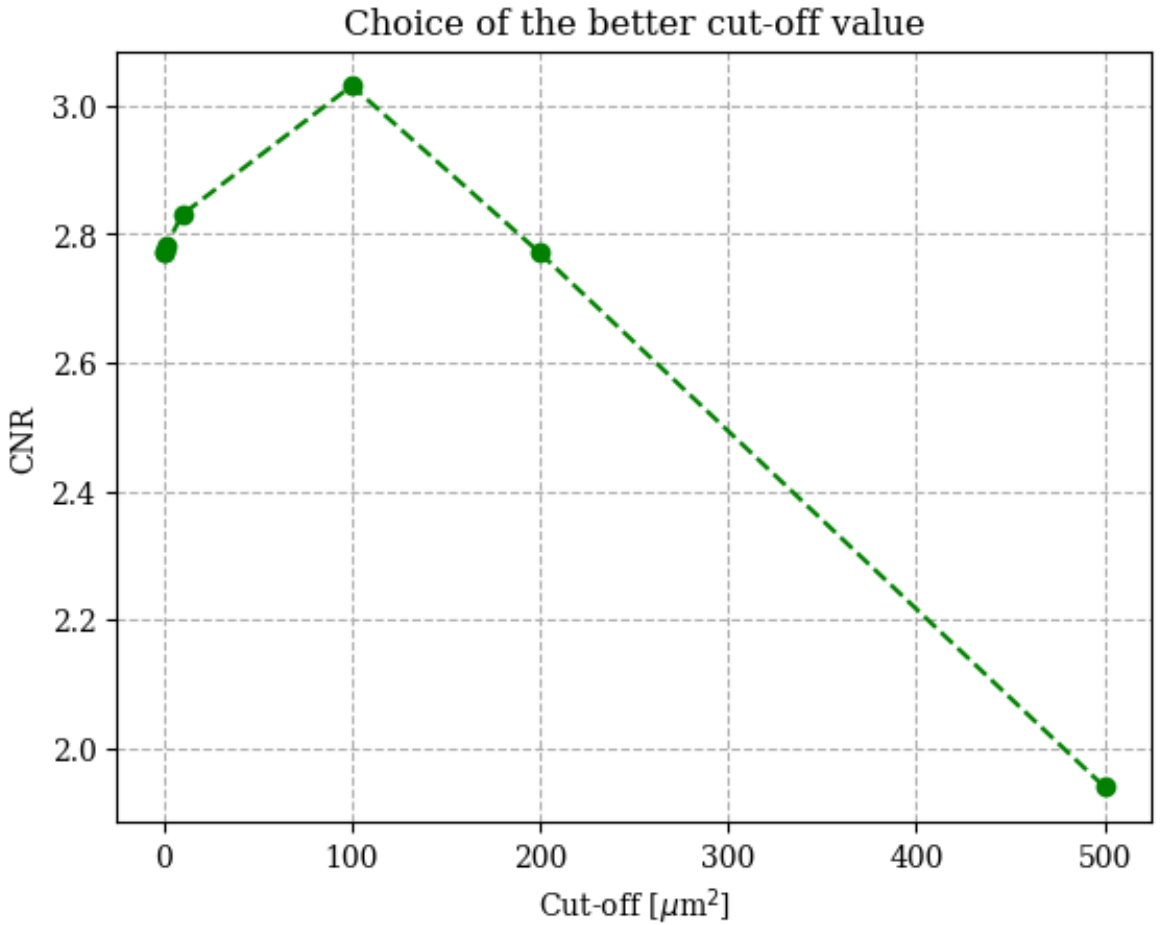

Cut-off optimization based in the best CNR value in the phase image

Results

In-line and SBI phase image

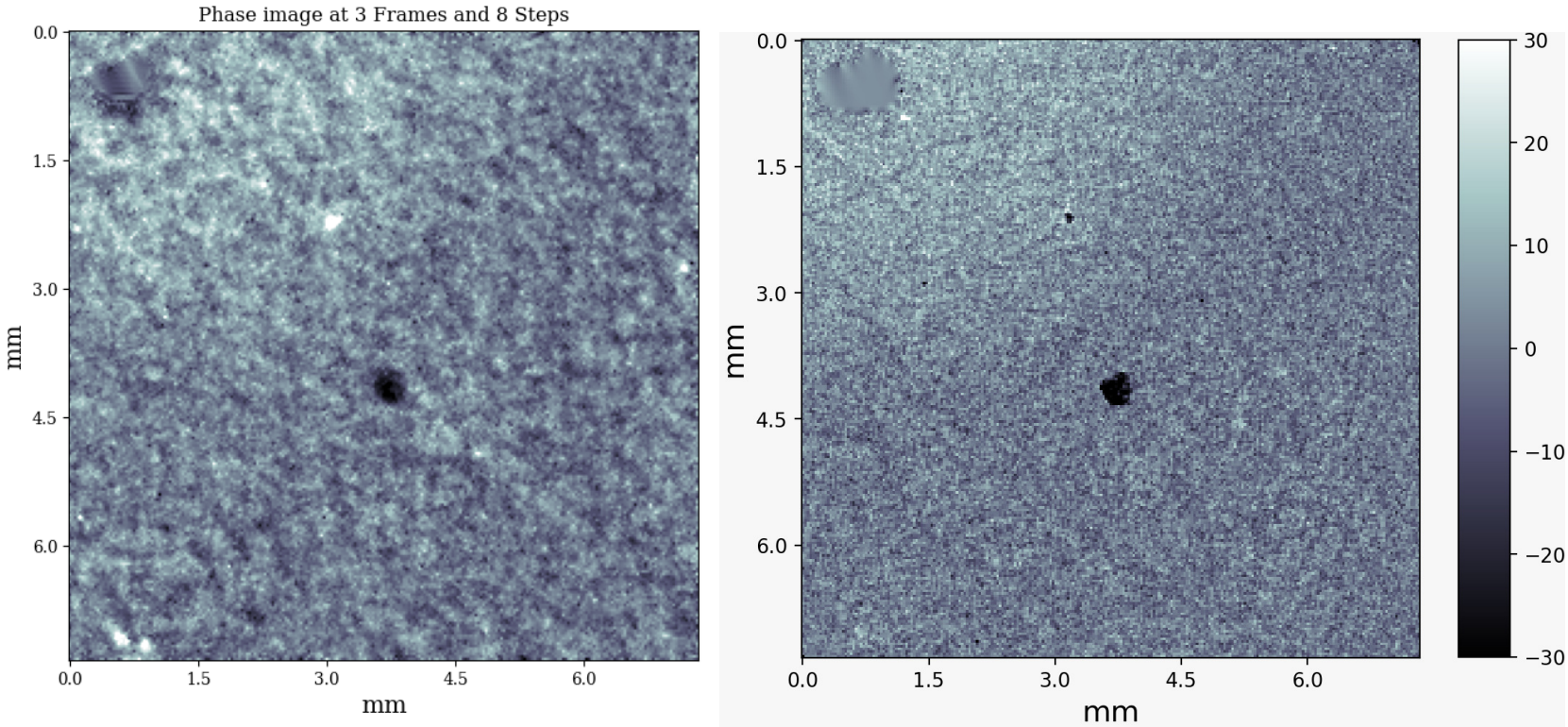

Phase signal retrieved with $E_{eff} = 17keV$, $\gamma = 344.8$ and M=1.8. **Left:**Phase image using SBI method CNR = 3.78. **Rigth:**Phase image using In-line method CNR=5.73

CNR Curves and Dose

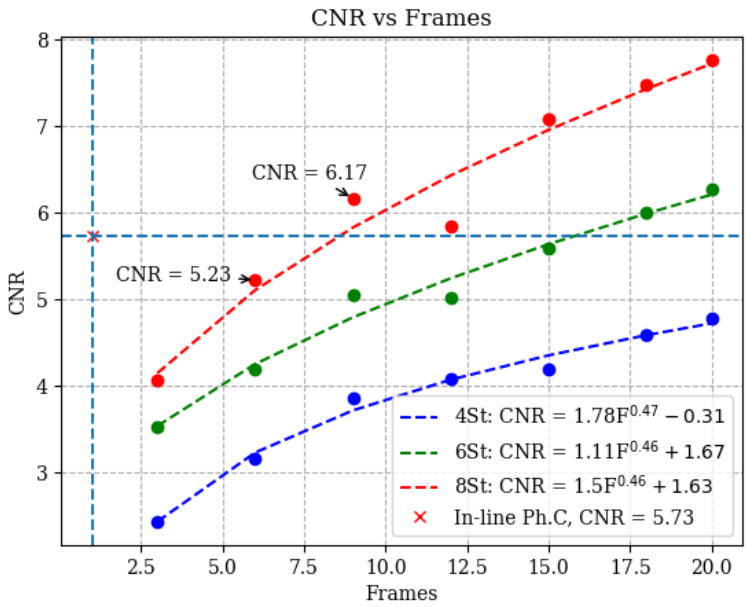

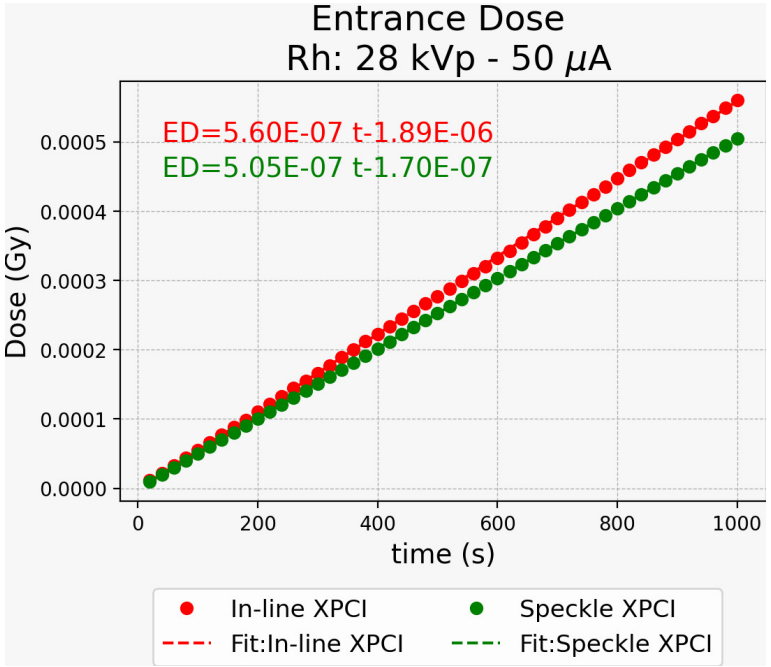

Contrast-to-Noise ratio at different frames and steps

$$CNR = \frac{|I_{BGK} - I_{samp}|}{\sigma_{BKG}} \quad (15)$$

Phase images using 6 and 8 frames

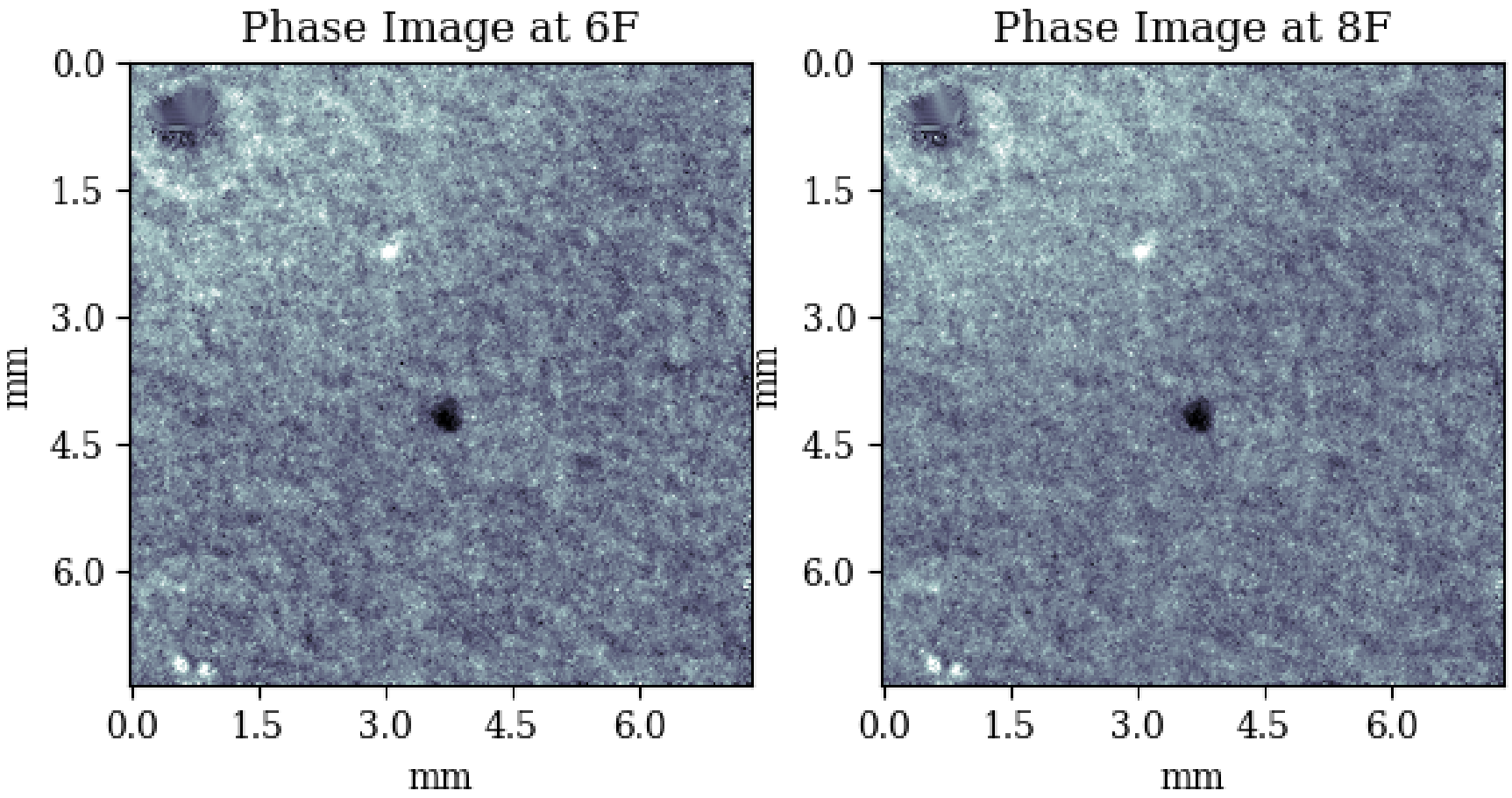

Phase images from SBI method using 6 and 8 franes

Laplacian image

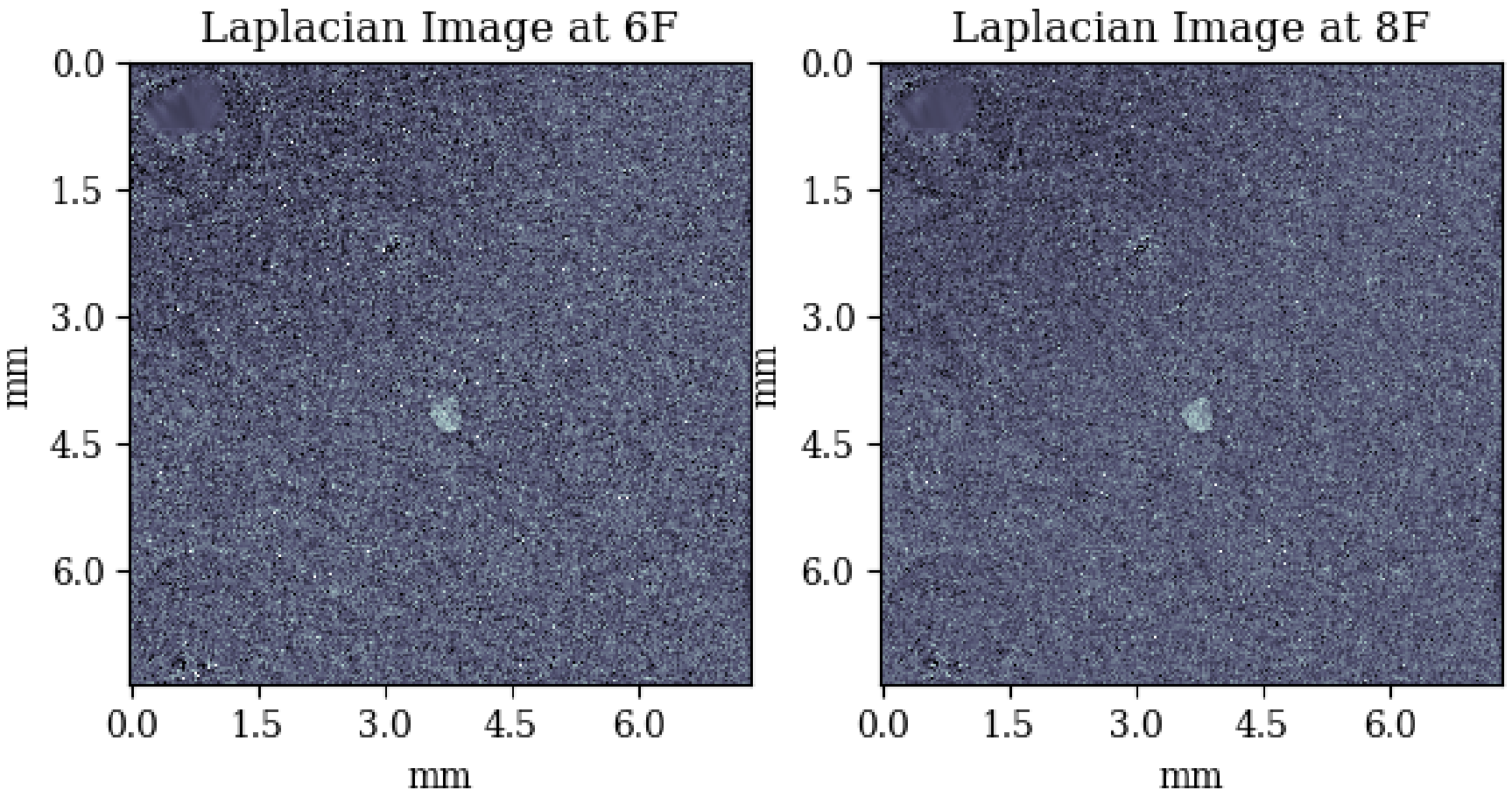

Laplacian image using 6 and 8 frames.

Dark-field image

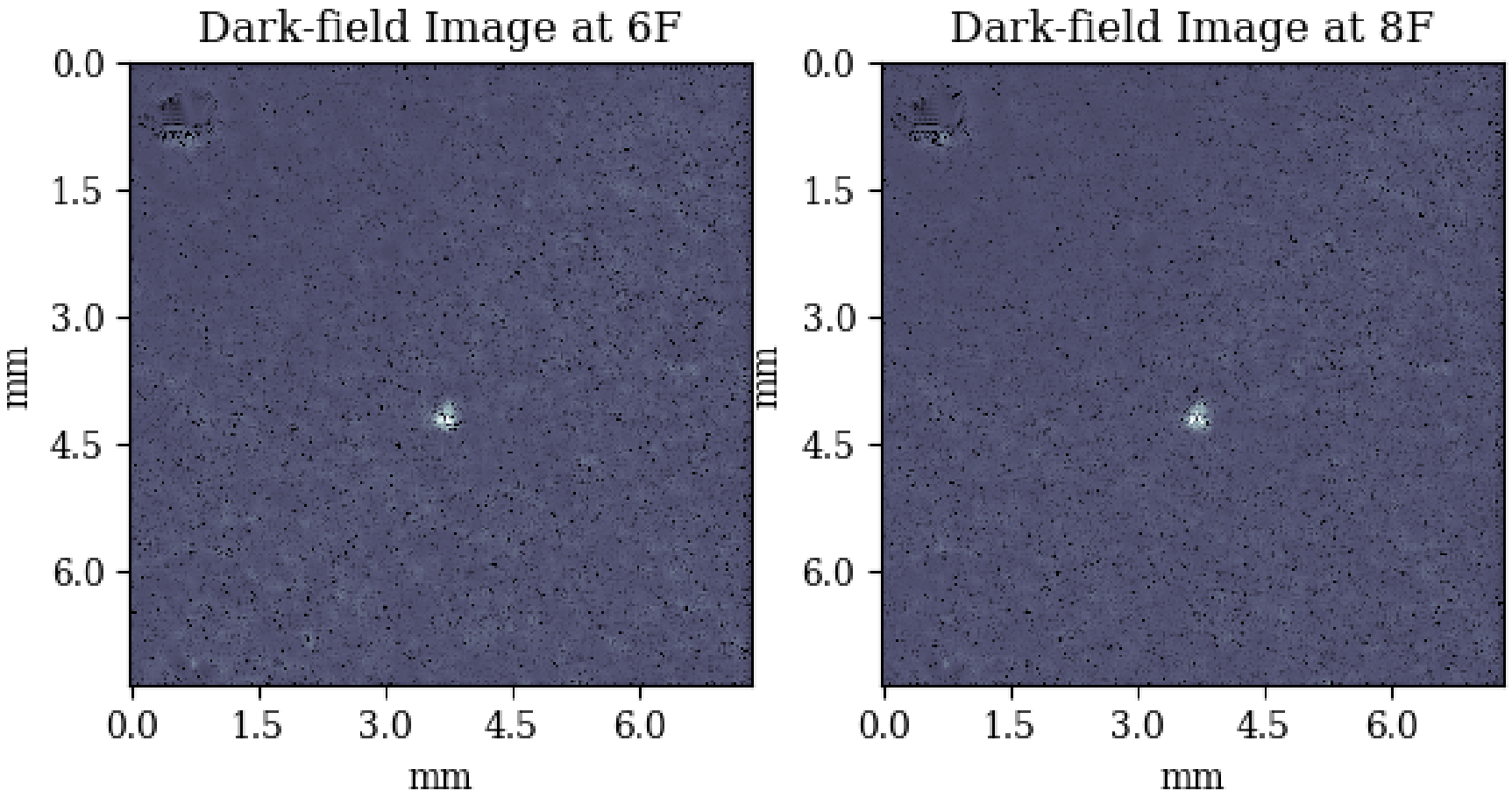

Dark-field image using 6 and 8 frames.

Conclusions

- In-line method offers higher CNR respect to the SBI method, this because was used low number of frames to be comparable one method respect to the other.

- SBI method can be used as a complementary method in the detection of breast lesions due to the additional signals it offers, such as the laplacian and drak-field images.

- Using photon-counting detectors it is possible to estimate the dose received by a sample and resolve an image using specific energies.

THANK YOU FOR YOUR ATTENTION

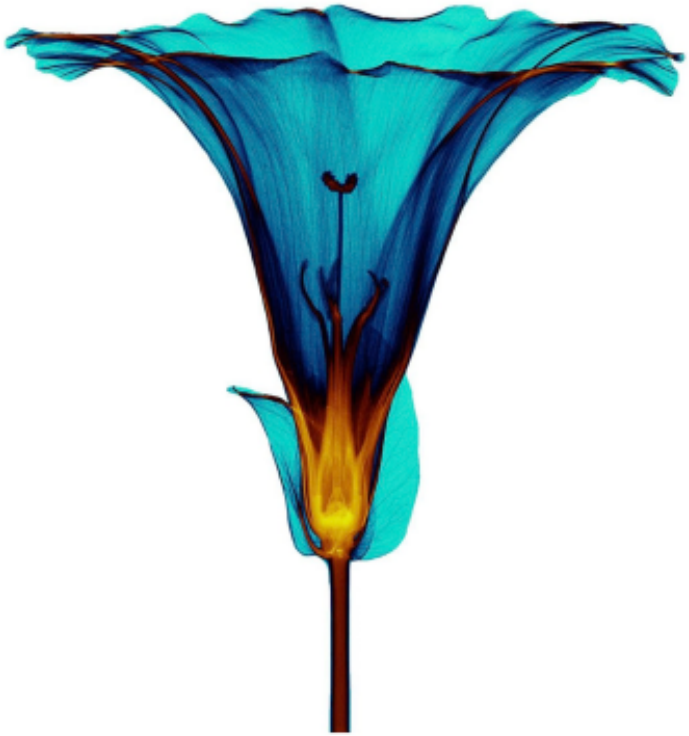

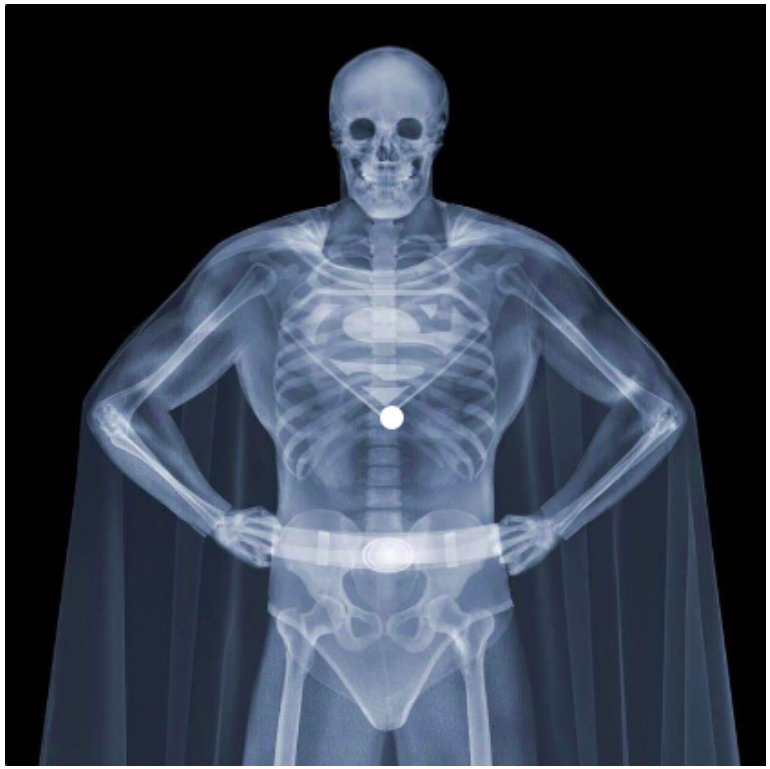

taken from [21],[22]

References

[1] https://medipix.web.cern.ch/news/news/medipix/first-3d-colour-x-ray-human-using-cern-technology.
[2] Turner, J. E. (2008).Atoms, radiation, and radiation protection. John Wiley and Sons.
[3] http://ts-imaging.science.unimelb.edu.au/Services/Simple/.
[4]Gureyev, T. E., Paganin, D. M., Arhatari, B., Taba, S. T., Lewis, S., Brennan, P. C., Quiney, H. M. (2020). Dark-field signal extraction in propagation-based phase-contrast imaging. Physics in Medicine Biology, 65(21), 215029.
[5]Brombal, L., Golosio, B., Arfelli, F., Bonazza, D., Contillo, A., Delogu, P., Longo, R. (2018, March). Monochromatic breast CT: absorption and phase-retrieved images. In Medical Imaging 2018: Physics of Medical Imaging (Vol. 10573, pp. 504-515). SPIE.
[6] S.J. Alloo and et al. Multimodal intrinsic speckle-tracking (mist) to extract images of rapidly- varying diffuse x-ray dark-field. Sci Rep, 14:5424, 2023.
[7] Vittorio Di Trapani, Sara Savatovic, Fabio De Marco, Ginevra Lautizi, Marco Margini, and Pierre Thibault. Speckle-based imaging (SBI) applications with spectral photon counting detectors at the newly established optimato (optimal imaging and tomography) laboratory. Journal of Instrumentation, 19(01):C01018, 2024.

References

[8] Gureyev, T. E., Paganin, D. M., Arhatari, B., Taba, S. T., Lewis, S., Brennan, P. C., and Quiney, H. M. (2020). Dark-field signal extraction in propagation-based phase-contrast imaging. Physics in Medicine and Biology, 65(21), 215029.
[9] Yu, F., Li, K., Wang, F., Zhang, H., Ju, X., Xu, M., abd Xiao, T. (2021). Double-exposure method for speckle-tracking x-ray phase-contrast microtomography. Journal of Applied Physics, 129(7).
[10] Brombal, L., Golosio, B., Arfelli, F., Bonazza, D., Contillo, A., Delogu, P.,and Longo, R. (2018, March). Monochromatic breast CT: absorption and phase-retrieved images. In Medical Imaging 2018: Physics of Medical Imaging (Vol. 10573, pp. 504-515). SPIE.
[11] Kulpe, S., Dierolf, M., Günther, B., Busse, M., Achterhold, K., Gleich, B., Pfeiffer, D. (2019). K-edge subtraction computed tomography with a compact synchrotron X-ray source. Scientific reports, 9(1), 13332.
[12] Savatović, S., Zdora, M. C., De Marco, F., Bikis, C., Olbinado, M., Rack, A., and Zanette, I. (2024). Multi-resolution X-ray phase-contrast and dark-field tomography of human cerebellum with near-field speckles. Biomedical Optics Express, 15(1), 142-161.
[13] Zdora, M. C., Zanette, I., Walker, T., Phillips, N. W., Smith, R., Deyhle, H., and Thibault, P. (2020). X-ray phase imaging with the unified modulated pattern analysis of near-field speckles at a laboratory source. Applied optics, 59(8), 2270-2275.

References

[14]Pavlov, K. M., Li, H., Paganin, D. M., Berujon, S., Rougé-Labriet, H., and Brun, E. (2020). Single-shot x-ray speckle-based imaging of a single-material object. Physical Review Applied, 13(5), 054023.
[16] Walsh, M. F., Nik, S. J., Procz, S., Pichotka, M., Bell, S. T., Bateman, C. J., Butler, P. H. (2013). Spectral CT data acquisition with Medipix3. 1. Journal of Instrumentation, 8(10), P10012.
[17] Ballabriga, R., Campbell, M., Heijne, E., Llopart, X., Tlustos, L., and Wong, W. (2011). Medipix3: A 64 k pixel detector readout chip working in single photon counting mode with improved spectrometric performance. Nuclear Instruments and Methods in Physics Research Section A: Accelerators, Spectrometers, Detectors and Associated Equipment, 633, S15-S18.
[18]Ballabriga, R., Blaj, G., Campbell, M., Fiederle, M., Greiffenberg, D., Heijne, E. H. M., and Wong, W. (2011). Characterization of the Medipix3 pixel readout chip. Journal of Instrumentation, 6(01), C01052.
[19]https://medlineplus.gov/xrays.html
[20]Gureyev, T. E., Mayo, S. C., Myers, D. E., Nesterets, Y., Paganin, D. M., Pogany, A., Wilkins, S. W. (2009). Refracting Röntgen's rays: propagation-based x-ray phase contrast for biomedical imaging. Journal of Applied Physics, 105(10).